Electronic Supplementary Material (ESI) for ChemComm.
This journal is © The Royal Society of Chemistry 2024

Electronic Supplementary Information

AIE-based fluorescent probe to detect peroxynitrite levels in human serum and its cellular imaging

Jaewon Kim,[‡a] Jiyoung Yoo,[‡a] Byungkook Kim,[‡a] Kyung-Woo Lee,[‡a] Sunghyun Kim,[b] Sukwon Hong[*b] and Jong Seung Kim[*a]

[a] Department of Chemistry, Korea University, Seoul 02841, Korea

[b] Department of Chemistry, Gwangju Institute of Science and Technology, Gwangju 61005, Korea

[*] Corresponding: shong@gist.ac.kr (SH), jongskim@korea.ac.kr (JSK)

‡ These authors contributed equally.

Table of contents

1. Experimental Section

1.1. General information and materials

Unless otherwise noted, all the materials used for the synthesis were purchased from the commercial suppliers. 4-Bromo-1,8-naphthalic anhydride (TCI), 2-(2-Aminoethoxy)ethanol (TCI), Carbon tetrabromide (TCI), 4-formylphenylboronic acid (ACROS), Tetrakis(triphenylphosphine)palladium(0) (Aldrich), Potassium carbonate (Samchun), Triphenylphosphine (Alfa), Potassium iodide (Aldrich), Hydrazine (Aldrich), *N*,*N*-Dimethylhydrazine (Aldrich) were purchased and used without further purification. TLC Silica gel 60 F254, 0.25 mm (Merck) was used for analytical thin layer chromatography. Column chromatography was performed with silica gel 60 (Merck, 0.063~0.2 mm) as a stationary phase. ^{1}H and ^{13}C NMR spectra were collected in NMR solvents ($CDCl_3$) on a Bruker 500 MHz spectrometer. All chemical shifts are reported in ppm values using the peak of TMS as an internal reference. The mass spectra were collected on LC/MS-2020 Series (Shimadzu). Analytical or preparative high-performance liquid chromatography (HPLC) were performed using Young In ChroZen and the reverse phase column (SunFire®C18 OBD Prep Column, 5 μm, waters) was equipped. UV-Vis spectra were recorded on a JASCO V-750 spectrometer, and fluorescence spectra were obtained using a JASCO FP-8700 instrument. Stock solutions of **Mt-NI-Alde**, **Mt-NI-1** and **Mt-NI-2** were prepared in DMSO. All excitation and emission slit widths were set at 5 nm. The concentration of each of the samples was fixed at 10 μM in a total volume of 3 mL.

1.2. UV/Vis and Fluorescence spectroscopic method

All UV-vis absorption spectra were obtained using JASCO V-750 spectrophotometer. All fluorescence spectra were collected in JASCO FP-8500 spectrofluorometer. 10 mM stock solutions of **Mt-NI-Alde**, **Mt-NI-1**, **Mt-NI-2** in DMSO. $ONOO^-$ stock solution was prepared by a reported method. Briefly, under stirring at 0°C (Ice bath), a mixture of sodium nitrite ($NaNO_2$, 0.6 M) and hydrogen peroxide (H_2O_2, 0.7 M) was acidified with hydrochloric acid (HCl, 0.6 M), and sodium hydroxide (NaOH, 1.5 M) was added within 1-2 s to make the solution alkaline. The concentration of $ONOO^-$ was determined by measuring the absorption of the solution at 302 nm. The extinction coefficient of the $ONOO^-$ solution in 0.1M NaOH is 1670M^{-1} cm^{-1}, at 302 nm. Other ROS and RNS were prepared according to literature methods[1, 2]. The concentration of H_2O_2 was determined from the absorption with $\varepsilon = 43.6$ M^{-1} cm^{-1}, at 240 nm. The source of hypochlorous acid (HOCl) was commercial bleach. The concentration of HOCl was determined through spectrophotometrical analysis. The extinction coefficient of the HOCl solution in 0.1M NaOH is 350 M^{-1} cm^{-1}, at 292 nm. The concentration of ClO^- was determined from the absorption with $\varepsilon = 350$ M^{-1} cm^{-1}, at 292 nm. tert-Butyl hydroperoxide (TBHP) was prepared in deionized distilled water by diluting 70% TBHP. Peroxyl radical (ROO·) was generated from 2,2′-azobis(2-amidinopropane)dihydrochloride, which was firstly dissolved in deionizer water, and stirred at r.t. for 30 min. The hydroxyl radical (HO·) was generated by the Fenton reaction. To generate HO·, ferrous chloride was added in the presence of 10 equivalents of H_2O_2. The concentration of HO· was equal to that of Fe(II) concentration. Singlet oxygen ($^1O_2$) was chemically generated from the H_2O_2/NaOCl (1:1) system in physiological media. $O_2^{\bullet-}$ was prepared by adding potassium superoxide (KO_2) to dry dimethyl sulfoxide (DMSO) and stirring vigorously for 10 min. Nitric oxide (NO) was prepared by treating sulfuric acid

(3.6 M) solution with sodium nitrite solution (7.3 M) and its stock solution (2.0 mM) was prepared by bubbling NO into deoxygenated deionized water for 30 min. Nitrite (NO_2^-) and nitrate (NO_3^-) were prepared by dissolving sodium nitrite ($NaNO_2$) and sodium nitrate ($NaNO_3$) in deionized distilled water, respectively. Cysteine (Cys), homocysteine (Hcy), and glutathione (GSH) were prepared by dissolving L-cysteine, DL-homocysteine, and L-glutathione in deionized distilled water, respectively. Stock solutions for cations (10 mM) were prepared by dissolving chloride (Ca^{2+}, Fe^{2+}), perchlorate (Mg^{2+}), or sulfate (Cu^{2+}) salt in distilled water.

1.3. Synthesis of compound (Mt-NI-1, Mt-NI-2)

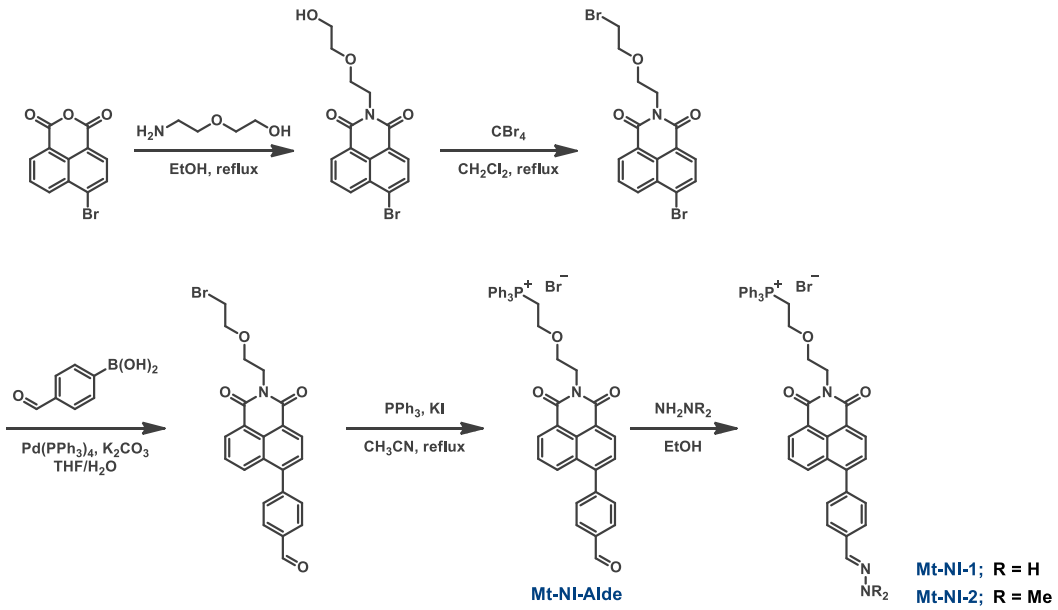

Scheme S1. Overall synthetic route of **Mt-NI-1** and **Mt-NI-2**

Synthesis of Compound 1

4-Bromo-1,8-naphthalic anhydride (2.6 g, 9.4 mmol, 1.0 equiv.) and 2-(2-Aminoethoxy)-ethanol (0.93 g, 9.4 mmol, 1.0 equiv.) were added to ethanol (50 mL) and stirred for 2 h in reflux condition. The resulting mixture was extracted with dichloromethane and the organic phase was washed with distilled water. After dried over Na_2SO_4, the solvent was evaporated by rotary evaporator and purified by column chromatography (eluent: DCM/MeOH = 95/5) then, bright yellow solid was afforded. ^{1}H NMR (500 MHz, $CDCl_3$) δ 8.65 (dd, *J* = 7.3, 0.9 Hz, 1H), 8.57 (dd, *J* = 8.5, 0.9 Hz, 1H), 8.41 (d, *J* = 7.9 Hz, 1H), 8.03 (d, *J* = 7.9 Hz, 1H), 7.84 (dd, *J* = 8.4, 7.4 Hz, 1H), 4.44 (t, *J* = 5.6 Hz, 2H), 3.86 (t, *J* = 5.6 Hz, 2H), 3.69 (d, *J* = 4.3 Hz, 2H), 3.67–3.64 (m, 2H), 2.41 (s, 1H) ppm; ^{13}C NMR (125 MHz, $CDCl_3$) δ 163.90, 133.45, 132.26, 131.43, 131.15, 130.57, 129.05, 128.12, 122.94, 122.07, 72.2, 68.3, 61.86, 39.66 ppm; ESI-MS (m/z); $[M+Na]^+$ calcd. for $C_{16}H_{14}BrNNaO_4$: 385.9998; found: 386.

Synthesis of Compound 2

A solution of **Compound 1** (300 mg, 0.82 mmol, 1.0 equiv.) and triphenylphosphine (645 mg, 2.46 mmol, 3.0 equiv.) in dichloromethane was added dropwise to a solution of carbon tetrabromide (815 mg, 2.46 mmol, 3.0 equiv.) in dichloromethane at 0°C. The reaction mixture was stirred for 3 h at room temperature. The mixture was extracted with dichloromethane and distilled water and evaporated by rotary evaporator. The mixed product was purified by gradient flash column chromatography with silica gel (eluent: DCM → DCM/MeOH = 97/3). ^{1}H NMR (500 MHz, $CDCl_3$) δ 10.14 (s, 1H), 8.70–8.58 (m, 2H), 8.17 (dd, *J* = 8.5, 1.0 Hz, 1H), 8.09–8.04 (m, 2H), 7.74–7.65 (m, 4H), 4.45 (t, *J* = 6.0 Hz, 2H), 3.85 (dt, *J* = 13.8, 6.1 Hz, 4H), 3.42 (t, *J* = 6.2 Hz, 2H) ppm; ^{13}C NMR (125 MHz, CDCl3) δ 163.71, 133.39, 132.16, 131.35, 131.14, 130.69, 130.40, 129.11, 128.10,

123.05, 122.18, 70.60, 67.83, 39.22, 30.36 ppm; ESI-MS (m/z); $[M+2(H_2O)+H]^+$ calcd. for $C_{16}H_{17}Br_2NNaO_5$: 483.9366; found: 482.

Synthesis of Compound 3

Compound 2 (212 mg, 0.496 mmol, 1.0 equiv.) and 4-formylphenylboronic acid (149 mg, 0.992 mmol, 2.0 equiv.) were dissolved into 10 mL of tetrahydrofuran, and then 3 mL of 2.0 M potassium carbonate solution was added. The mixed solution was degassed with argon gas for 20 min and then a catalytic amount of $Pd(PPh_3)_4$ was added. The mixture was stirred overnight upper than the boiling point of tetrahydrafuran under argon gas. After the reaction, the mixed solution was cooled and extracted with dichloromethane and distilled water. The organic part is dried over anhydrous Na_2SO_4 and evaporated with rotary evaporator. The mixed product was purified by flash column chromatography with silica gel (eluent: DCM/MeOH = 99.5/0.5). ^{1}H NMR (500 MHz, $CDCl_3$) δ 10.17 (s, 2H), 8.71–8.62 (m, 4H), 8.22–8.17 (m, 2H), 8.14–8.05 (m, 4H), 7.77–7.68 (m, 8H), 4.48 (t, *J* = 6.0 Hz, 4H), 3.88 (dt, *J* = 14.5, 6.1 Hz, 8H), 3.44 (t, *J* = 6.2 Hz, 4H), 1.76 (s, 1H) ppm; ^{13}C NMR (125 MHz, $CDCl_3$) δ 191.61, 164.20, 163.99, 145.28, 144.89, 136.20, 132.07, 131.52, 130.80, 130.63, 129.96, 129.75, 128.74, 127.86, 127.31, 122.97, 122.48, 70.61, 67.89, 39.19, 30.40 ppm; ESI-MS (m/z) $[M+3(H_2O)+H]^+$ calcd. for $C_{23}H_{25}BrNO_7$: 506.0809; found: 508.

Synthesis of Mt-NI-Alde

Compound 3 (173 mg, 0.382 mmol, 1.0 equiv.) and Triphenylphosphine (501 mg, 1.91 mmol, 5.0 equiv.) were added to 30 mL of acetonitrile solvent and stirred for 5 d in reflux condition. The reaction mixture was extracted with dichloromethane and distilled water. For better separation, diluted hydrobromic acid was added around 3 to 5 droplets. The organic part is dried over anhydrous Na_2SO_4 and

evaporated with rotary evaporator. Due to the charged product makes difficult to conduct flash column chromatography, packing of silica gel was around 5-cm-height. The mixed product was purified by gradient flash column chromatography with silica gel (eluent: DCM/MeOH = 99/1 → 97/3 → 95/5).

^{1}H NMR (500 MHz, $CDCl_3$) δ 10.18–10.14 (m, 1H), 8.68–8.57 (m, 2H), 8.21 (d, J = 8.5 Hz, 1H), 8.09 (d, J = 7.9 Hz, 2H), 7.84 (dd, J = 12.9, 8.2 Hz, 6H), 7.73 (dt, J = 12.9, 8.1 Hz, 8H), 7.64 (td, J = 7.9, 3.2 Hz, 6H), 4.22 (dt, J = 11.5, 5.6 Hz, 2H), 4.13 (t, J = 6.0 Hz, 2H), 4.00 (t, J = 5.6 Hz, 1H), 3.95 (t, J = 5.6 Hz, 1H), 3.47 (t, J = 6.0 Hz, 2H) ppm; ^{13}C NMR (125 MHz, $CDCl_3$) δ 191.73, 163.88, 163.68, 145.50, 144.62, 136.19, 134.70, 133.92, 132.30, 131.51, 130.81, 130.61, 130.27 – 129.93, 129.70, 128.59, 127.91, 127.40, 122.63, 122.12, 119.12, 118.43, 68.03, 64.08, 53.51, 38.92, 25.54, 25.11 ppm; ESI-MS (m/z) $[M]^+$ calcd. for $C_{41}H_{33}NO_4P$: 634.2142; found: 634.

Synthesis of Mt-NI-1

Mt-NI-Alde (50 mg, 53.1 μmol, 1.0 equiv.) and hydrazine (5.3 μL, 106 μmol, 2.0 equiv.) were mixed in 10 mL ethanol for 2 h at room temperature. After the reaction, the mixed solution was cooled and extracted with dichloromethane and distilled water. The organic part is dried over anhydrous Na_2SO_4 and evaporated with rotary evaporator. ^{1}H NMR (500 MHz, $CDCl_3$) δ 8.61–8.55 (m, 2H), 8.31 (dd, J = 8.5, 1.0 Hz, 1H), 7.90–7.78 (m, 6H), 7.77–7.66 (m, 8H), 7.64–7.57 (m, 6H), 7.51 (d, J = 8.2 Hz, 2H), 5.86–5.56 (m, 2H), 4.29–4.19 (m, 2H), 4.12 (t, J = 6.0 Hz, 2H), 4.00 (s, 1H), 3.95 (s, 1H), 3.47 (t, J = 6.0 Hz, 2H) ppm; ^{13}C NMR (125 MHz, $CDCl_3$) δ 163.99, 163.89, 146.83, 141.61, 138.52, 135.82, 134.61, 134.01, 132.90, 131.37, 130.96, 130.29, 129.84, 128.73, 127.78, 126.96, 126.38, 122.57, 121.42, 119.28, 118.59, 68.05, 64.21, 53.45, 38.90, 25.58, 25.16 ppm; ESI-MS (m/z) $[M]^+$ calcd. for $C_{41}H_{35}N_3O_3P$: 648.2411; found: 648.

Synthesis of Mt-NI-2

Mt-NI-Alde and *N*, *N'*-dimethylhydrazine were mixed in 10 mL ethanol for 2 h at room temperature. After the reaction, the mixed solution was cooled and extracted with dichloromethane and distilled water. The organic part is dried over anhydrous Na_2SO_4 and evaporated with rotary evaporator. ^{1}H NMR (500 MHz, $CDCl_3$) δ 8.59–8.54 (m, 2H), 8.34 (dd, J = 8.5, 1.0 Hz, 1H), 7.81 (ddd, J = 12.9, 5.2, 3.4 Hz, 6H), 7.76–7.66 (m, 8H), 7.64–7.56 (m, 6H), 7.47 (d, J = 8.2 Hz, 2H), 7.30 (s, 1H), 4.17 (dt, J = 11.5, 5.7 Hz, 2H), 4.13 (t, J = 6.0 Hz, 2H), 4.00 (t, J = 5.6 Hz, 1H), 3.95 (t, J = 5.7 Hz, 1H), 3.48 (t, J = 6.0 Hz, 2H), 3.05 (s, 6H) ppm; ^{13}C NMR (125 MHz, $CDCl_3$) δ 164.13, 163.93, 147.25, 137.57, 137.08, 134.58, 134.00, 133.06, 131.31, 130.99, 130.79, 130.06, 128.78, 127.72, 126.82, 125.67, 122.55, 121.19, 119.30, 118.61, 68.07, 64.20, 53.43, 42.77, 38.89, 25.58, 25.16 ppm; ESI-MS (m/z) $[M]^+$ calcd. for $C_{43}H_{39}N_3O_3P$: 676.2724; found: 676.

1.4. Determination of the detection limit

The detection limit was determined from the fluorescence titration data based on a reported method. **Mt-NI-2** (10 μM) was titrated with different concentrations of peroxynitrite ($ONOO^-$), the linear relationship between the values of emission intensity at 450 nm and the concentration of $ONOO^-$ was fitted based on the fluorescence titration. Detection limit = 3σ/s Where σ is the standard deviation of the blank sample and 's' is the slope of the linear regression equation.

1.5. Water fraction (f_w)

The aggregation study was performed following previous research[3]. The DMF/water solvent system was used to confirm whether **Mt-NI-2** have AIE or ACQ property. **Mt-NI-2** displayed absorption and emission maxima at

approximately 361 nm and 450 nm respectively. The fluorescence spectra were recorded by taking different f_w (0, 20, 40, 60, 80, 99.9%) in DMF.

1.6. Measurement of two-photon fluorescence excitation (TPE) cross section

The method of measurement was modified based on previously reported protocol[4]. The two-photon cross sections ($\eta_2\delta$) were determined using the femtosecond (fs) fluorescence measurement technique. **Mt-NI-Alde** of 5.0×10^{-5} M were excited by a mode-locked Ti:Sapphire pulsed femtosecond laser (Mai Tai HP, Spectra-Physics), and the two-photon excited fluorescence spectra were recorded with a Hitachi F-4600 fluorescence spectrophotometer. Rhodamine B of 1.0×10^{-5} M dissolved in MeOH was selected as the reference. The intensities of the two-photon fluorescence spectra of the reference and sample emitted at the same excitation wavelength were determined. The value of $\eta_2\delta$ was calculated using Eq:

$$\frac{\langle F(t)\rangle_{probe}}{\langle F(t)\rangle_{ref}} = \frac{\frac{1}{2}\phi\eta_2 C\delta \frac{g_p}{f_\tau}\frac{8n\langle P(t)\rangle_{probe}^{2}}{\pi}}{\frac{1}{2}\phi\eta_2 C\delta \frac{g_p}{f_\tau}\frac{8n\langle P(t)\rangle_{ref}^{2}}{\pi}}$$

Where η_2 and ϕ are the fluorescence quantum efficiency of the dye and the fluorescence collection efficiency of the measurement system, respectively. $\langle F(t)\rangle$ is time-averaged fluorescence photon flux. The numerical value of $g = g_p/(f\tau)$ for a mode-locked Ti:sapphire laser is approximately 10^5 ($f \sim 100$ MHz and $\tau \sim 100$ fs). δ is the two-photon cross sectional value and C is the concentration of the dye solution, n is there refractive index of the solution. $\langle P(t)\rangle$ is time-averaged incident power.

1.7. DFT calculation for sensing mechanism study

All the quantum-chemical calculations were done with the Gaussian 16 suite[5, 6]. The parameter referred to the previous work. The geometry optimizations of the chemical compounds were performed using time-dependent density functional theory (TD-DFT) with Becke's three-parameter hybrid exchange function with Lee-Yang-Parr gradient-corrected correlation functional (B3LYP) and 6-311G(d) basis set. No constraints to bonds/angles/dihedral angles were applied in the calculations and all atoms were free to optimize.

1.8. Cell lines and reagents

HeLa cells obtained from the Korean Cell Line Bank (Seoul, Korea) were cultured in RPMI 1640 media from HyClone (Chicago, IL, USA). Media were supplemented with 10% FBS (GIBCO, Grand Island, NY, USA) and 1% penicillin/streptomycin (GIBCO), and cells were maintained at 37 °C in a humidified atmosphere with 5% CO_2. LPS (Lipopolysaccharides) and IFN-γ human were purchased from Sigma-Aldrich; Merck KGaA, while PMA (Phorbol 12-myristate 13-acetate) was purchased from Thermo Fisher Scientific; MA; USA.

1.9. Cell viability assay

HeLa cells were seeded at a density of 5×10^3 cells per well in 96-well plates and allowed to adhere for at least 24 h. Following incubation, cells were treated with **Mt-NI-2** and **Mt-NI-Alde** or 1% DMSO as a control. Cell viability was then measured after 6 h using the Cellomax™ Cell Viability Kit (Precaregene, Hanam, Gyeonggi-do, Korea) according to the manufacturer's instructions. Subsequently, absorbance was measured at 450 nm using a Hidex Sense microplate reader (Hidex, Cranbourne, Victoria, AU). Triplicate assays were conducted for each condition, and cytotoxicity was expressed as a percentage relative to the control group. . The

experiment was repeated three times, and data were presented as mean values ± standard deviation (SD). Statistical significance was determined using a student's t-test and one or two-way ANOVA (GraphPad Prism8 software, CA, USA), with significance defined as *P < 0.05.

1.10. Cellular imaging

HeLa cells (2.0×10^4 per dish) were plated in 35-mm confocal glass bottom dishes allowed to adhere for 24 h. Following adherence, the cells were pretreated with LPS (1 μg/ml) and IFN-γ (200 μg/ml) in the media. After 12 h incubation, the cells were washed twice with fresh media, and 34 μM of PMA was additionally treated for 30 min before incubation with 5 μM of **Mt-NI-2**, after which fluorescence emission was recorded. Confocal laser scanning microscope (CLSM) images were acquired using an Olympus FV3000 confocal laser scanning microscope, with excitation and emission wavelengths set at 405 nm/480 nm. For mitochondria staining, 200 nM of MitoTracker® Deep Red FM (Invitrogen, CA, USA) was treated for 30 min before imaging (Ex: 644 nm/ Em: 665 nm). All the images and colocalization analysis were analyzed using Image J software (Rasband, W.S., ImageJ, U. S. National Institutes of Health, Bethesda, Maryland, USA, https://imagej.net/ij/, 1997-2018).

2. NMR and ESI-MS spectra

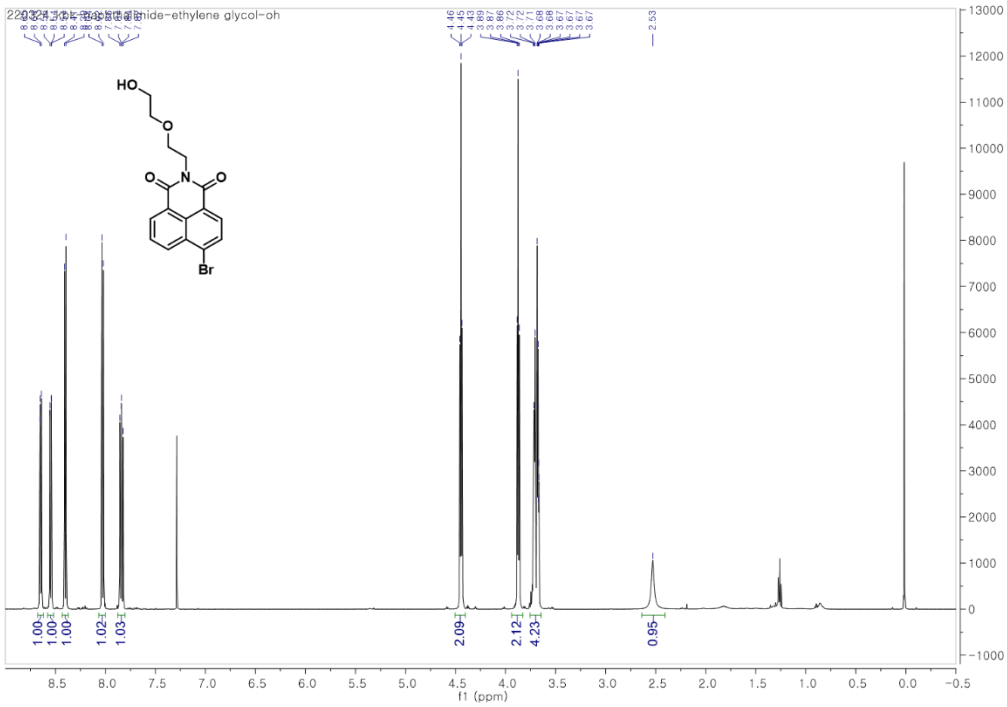

Figure S1. ^{1}H NMR ($CDCl_3$, 500 MHz) spectrum of Comound 1

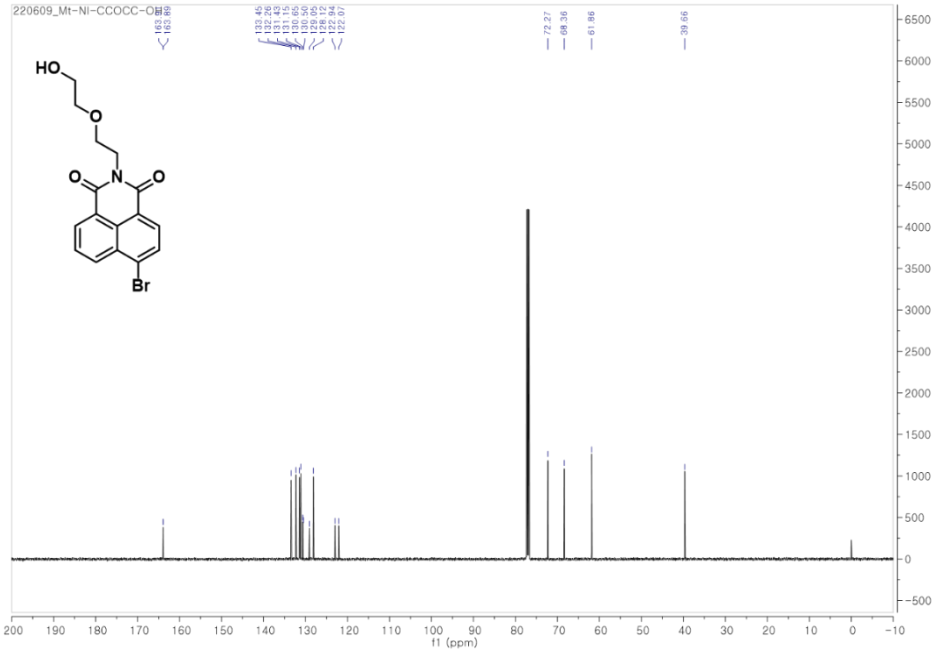

Figure S2. ^{13}C NMR ($CDCl_3$, 125 MHz) spectrum of Compound 1

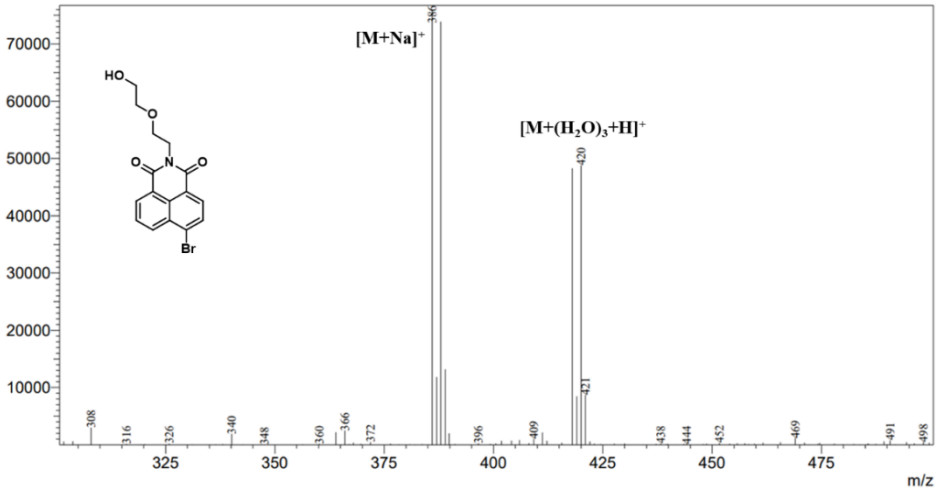

Figure S3. ESI-MS spectrum of Compound 1

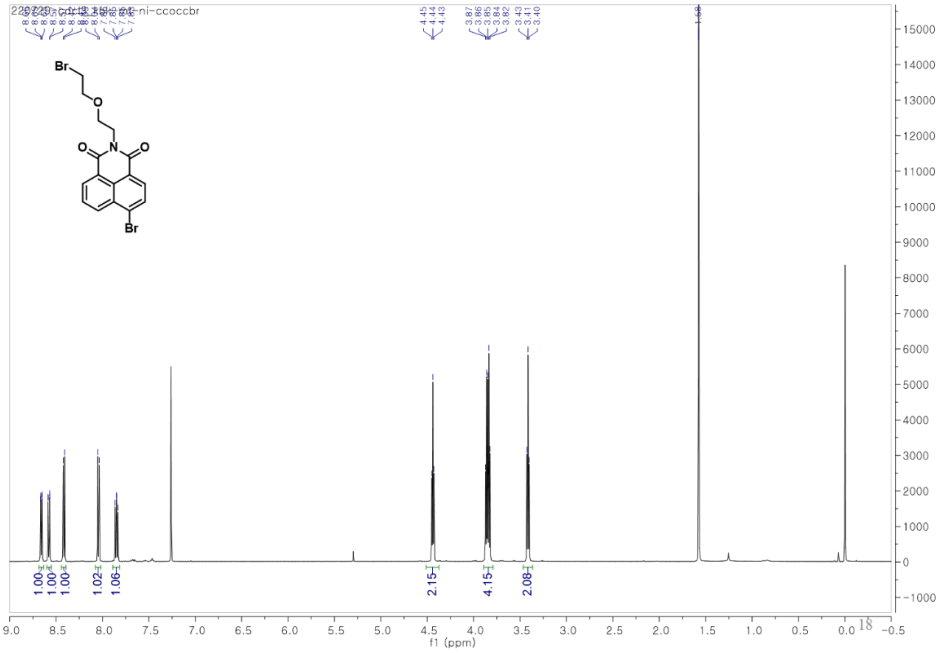

271

272 **Figure S4.** ^{1}H NMR ($CDCl_3$, 500 MHz) spectrum of Compound 2

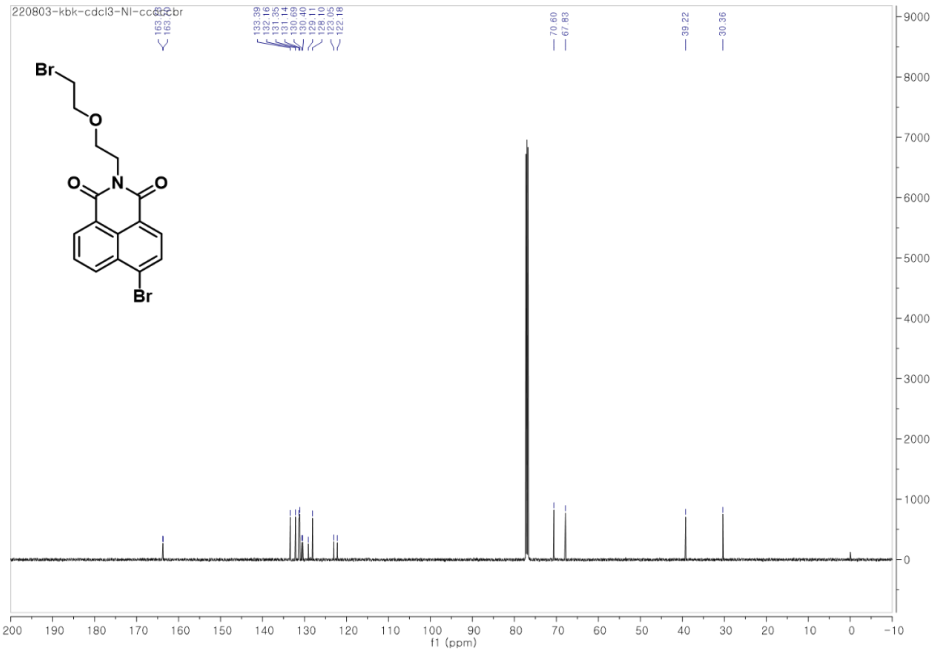

273

274 **Figure S5.** ^{13}C NMR ($CDCl_3$, 125 MHz) spectrum of Compound 2

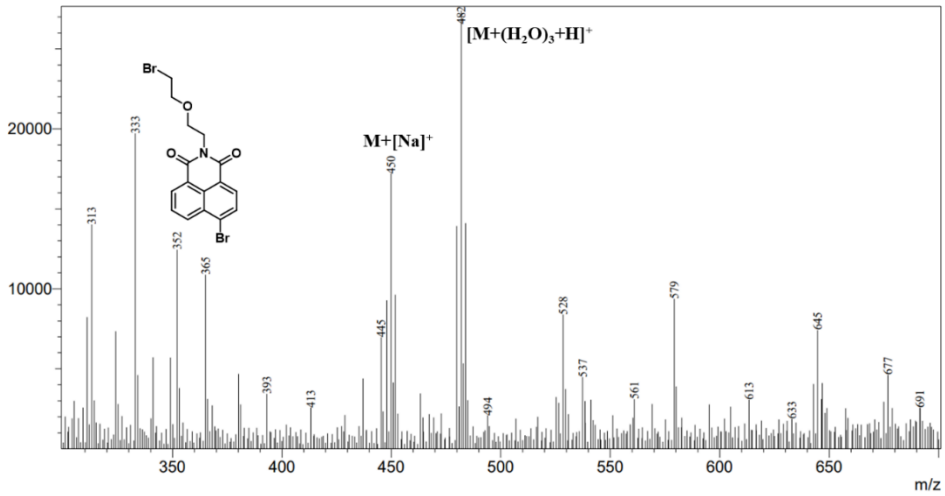

Figure S6. ESI-MS spectrum of Compound 2

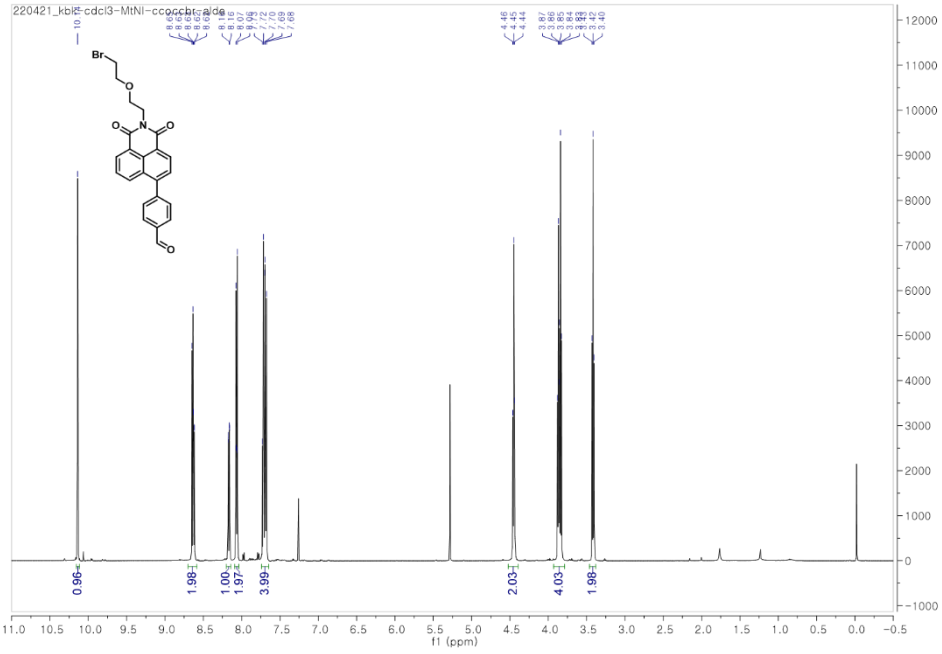

Figure S7. ^{1}H NMR ($CDCl_3$, 500 MHz) spectrum of Compound 3

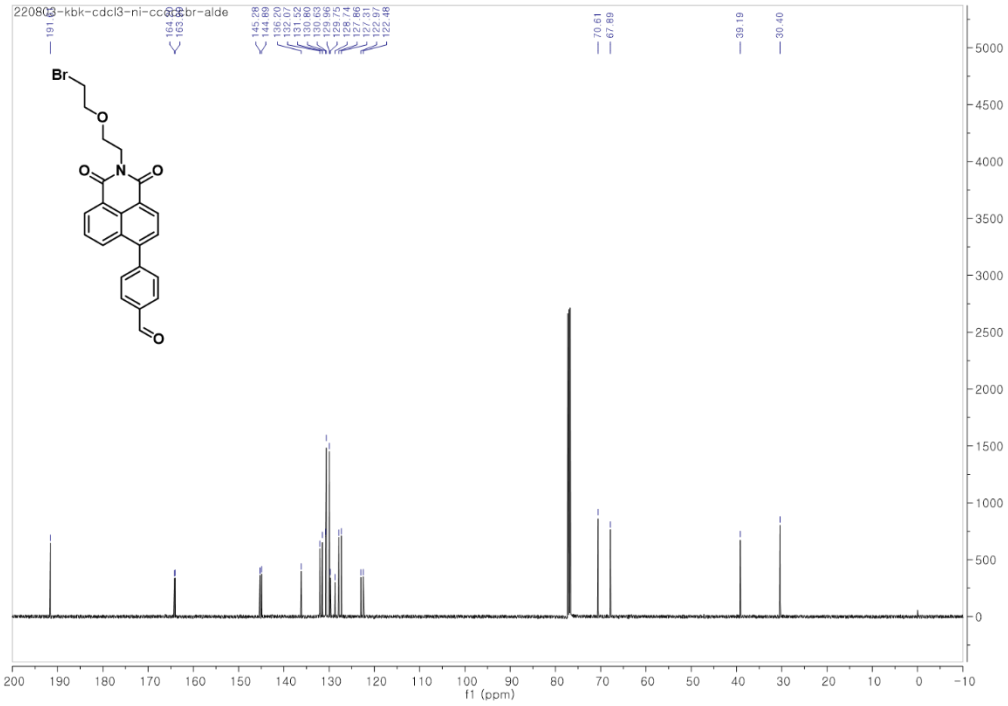

Figure S8. ^{13}C NMR ($CDCl_3$, 125 MHz) spectrum of Compound 3

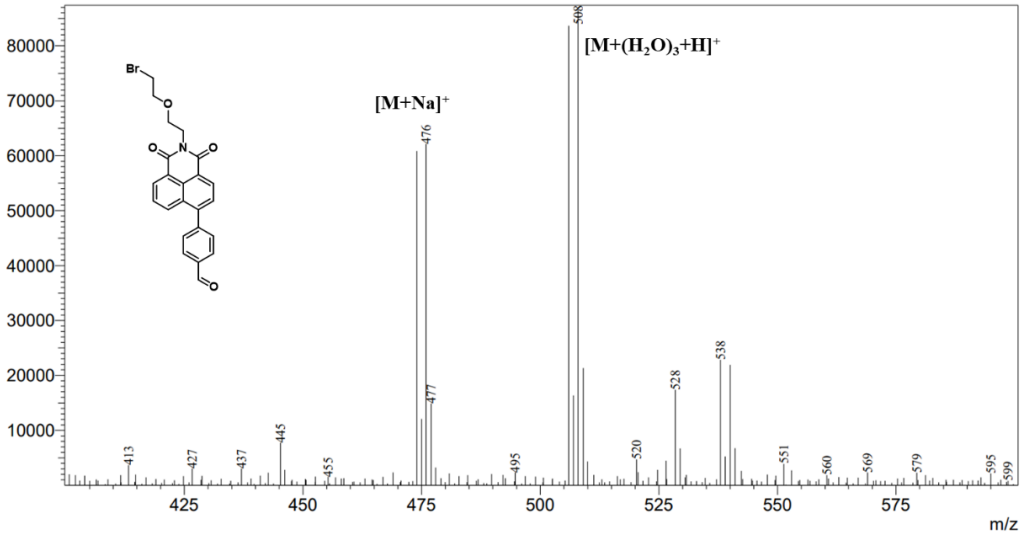

Figure S9. ESI-MS spectrum of Compound 3

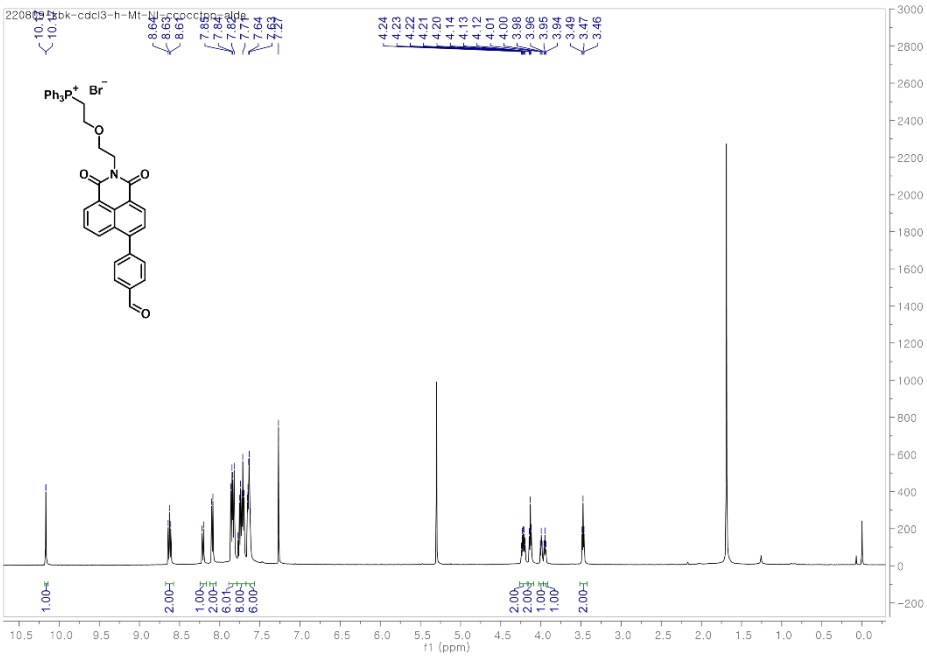

Figure S10. ^{1}H NMR ($CDCl_3$, 500 MHz) spectrum of **Mt-NI-Alde**

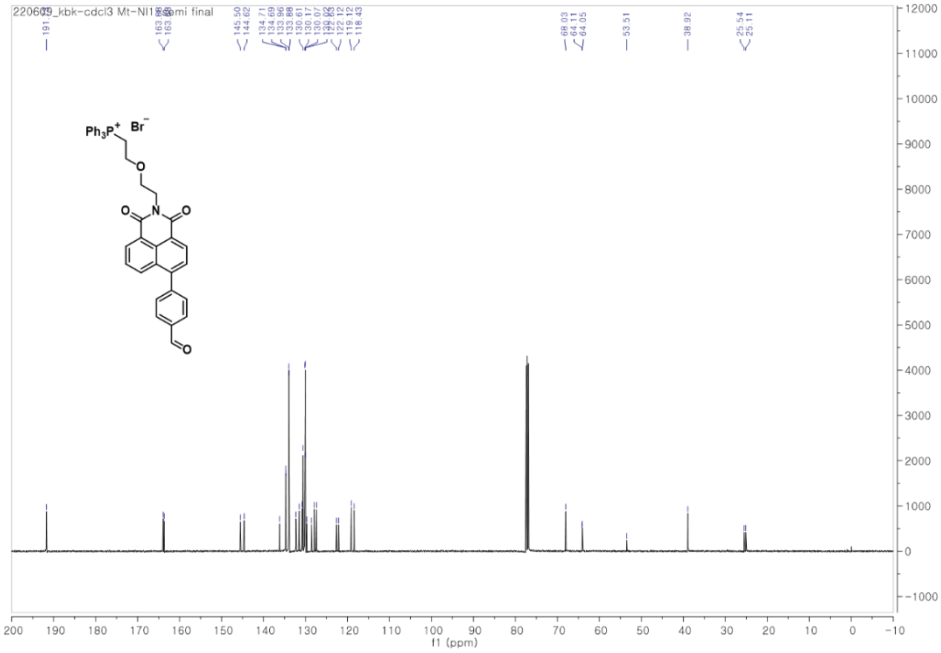

Figure S11. ^{13}C NMR ($CDCl_3$, 125 MHz) spectrum of **Mt-NI-Alde**

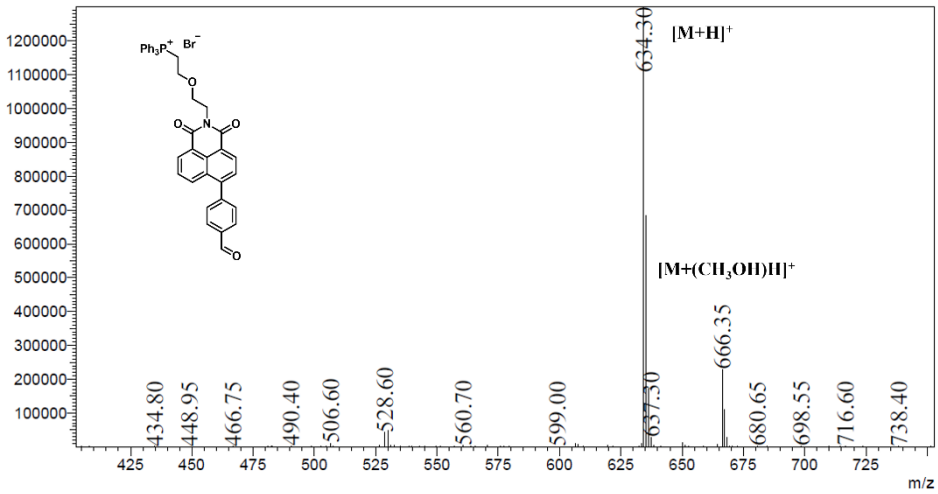

Figure S12. ESI-MS spectrum of **Mt-NI-Alde**

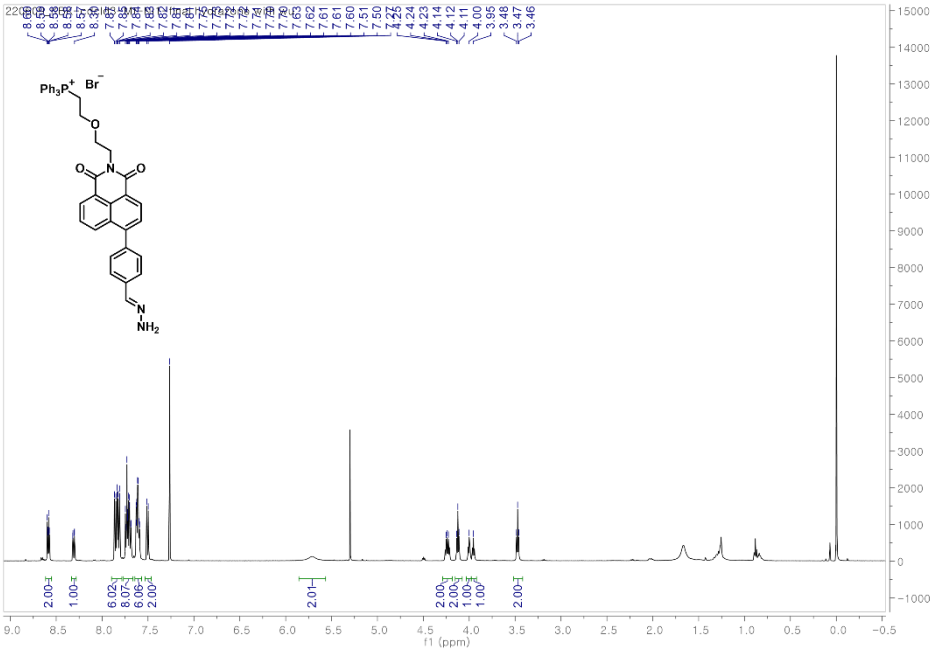

Figure S13. ^{1}H NMR ($CDCl_3$, 500 MHz) spectrum of **Mt-NI-1**

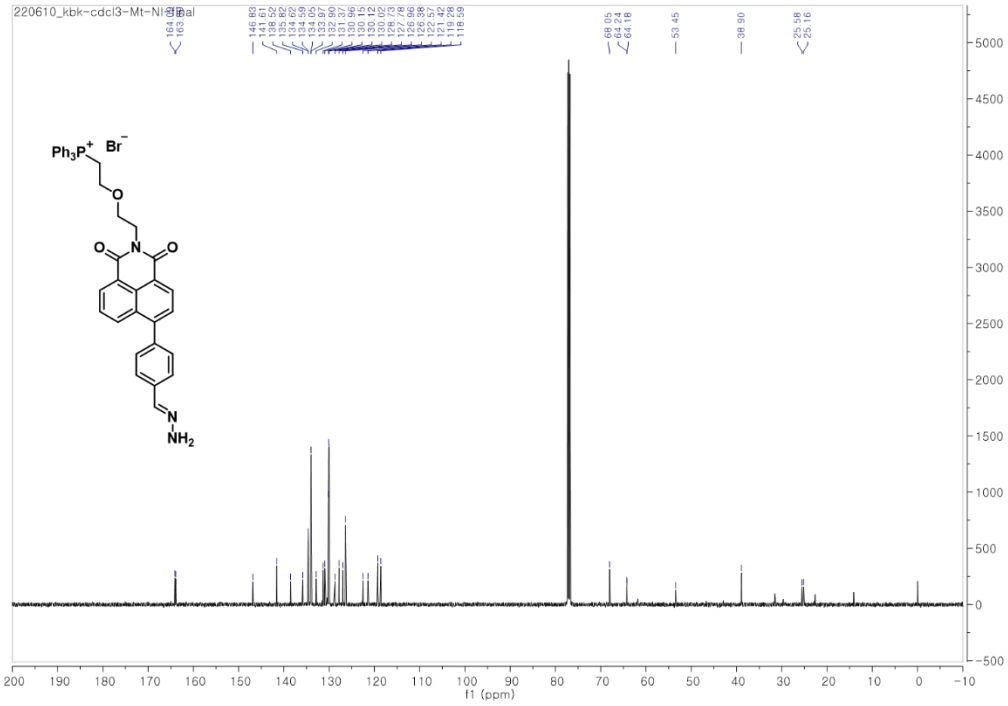

295

296 **Figure S14.** ^{13}C NMR ($CDCl_3$, 125 MHz) spectrum of **Mt-NI-1**

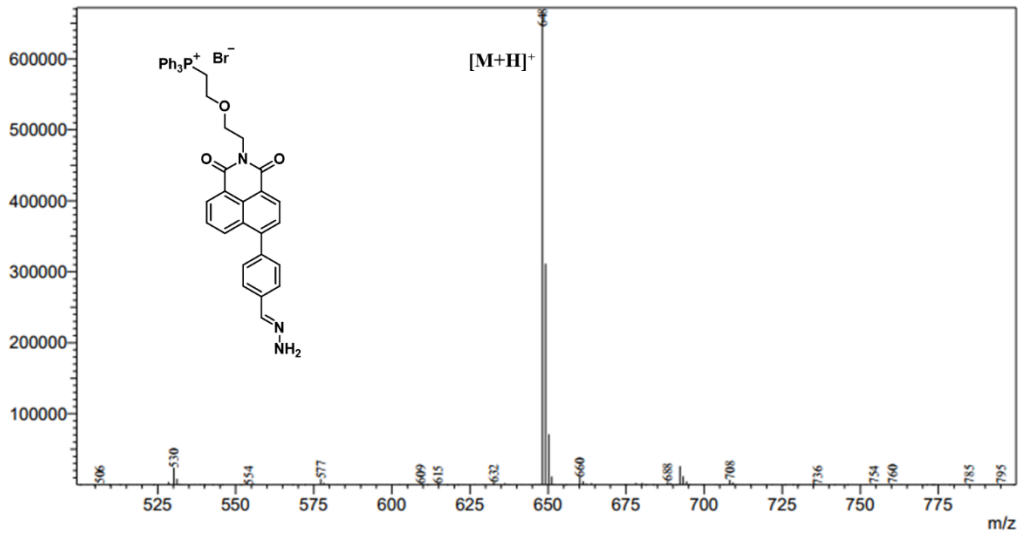

297

298 **Figure S15.** ESI-MS spectrum of **Mt-NI-1**

299

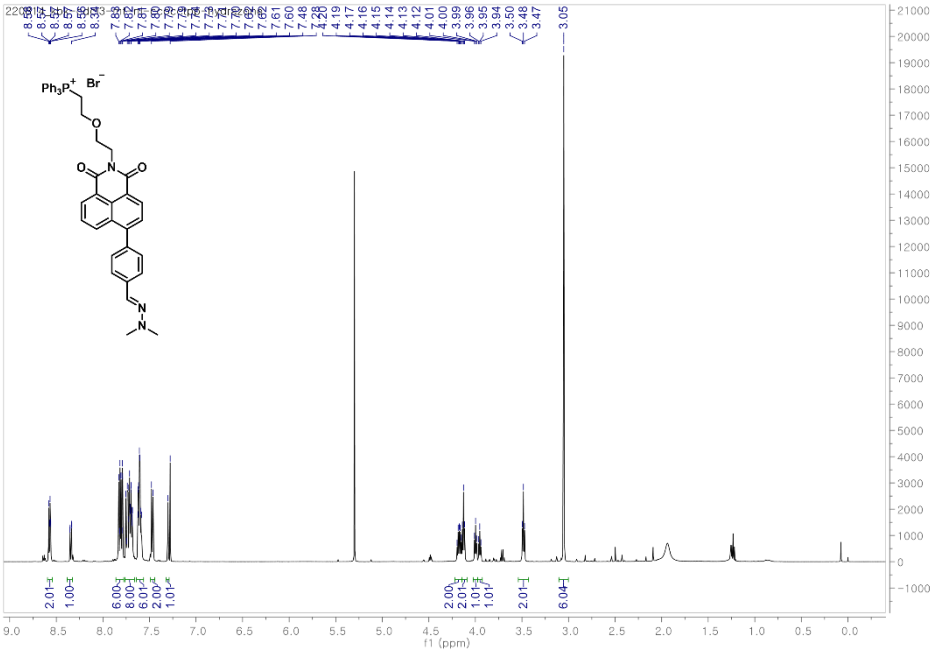

Figure S16. ^{1}H NMR ($CDCl_3$, 500 MHz) spectrum of **Mt-NI-2**

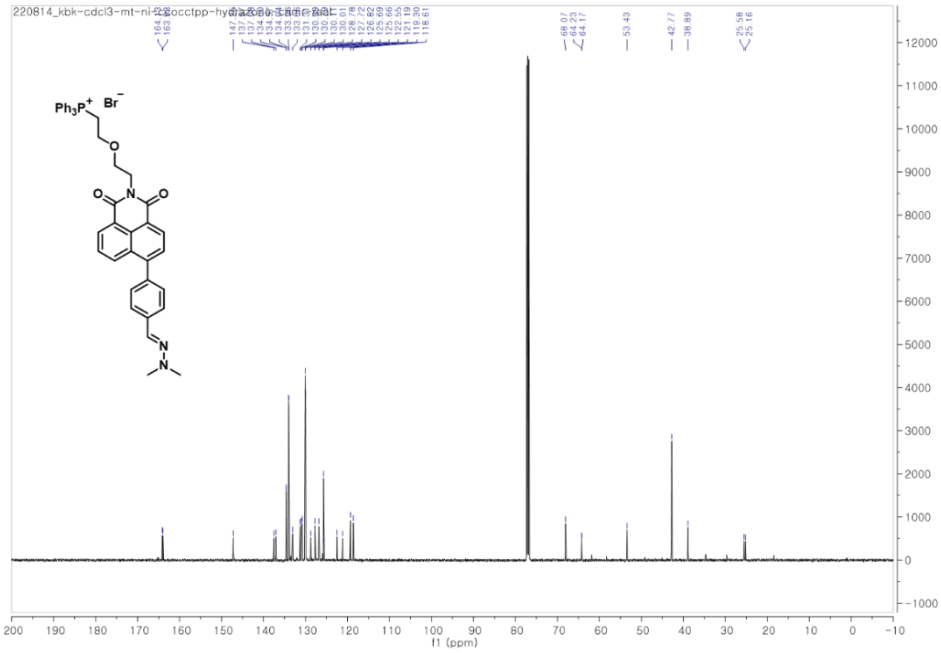

Figure S17. ^{13}C NMR ($CDCl_3$, 125 MHz) spectrum of **Mt-NI-2**

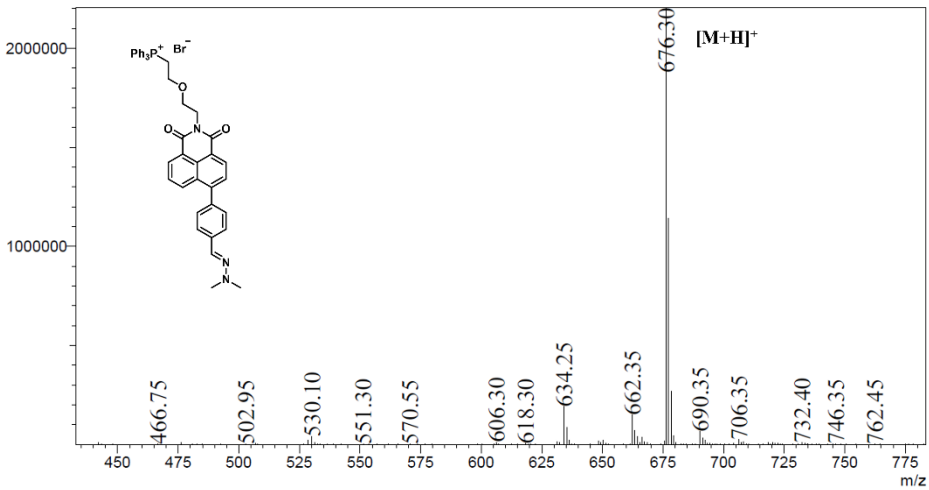

Figure S18. ESI-MS spectrum of **Mt-NI-2**

3. Solution test experiments

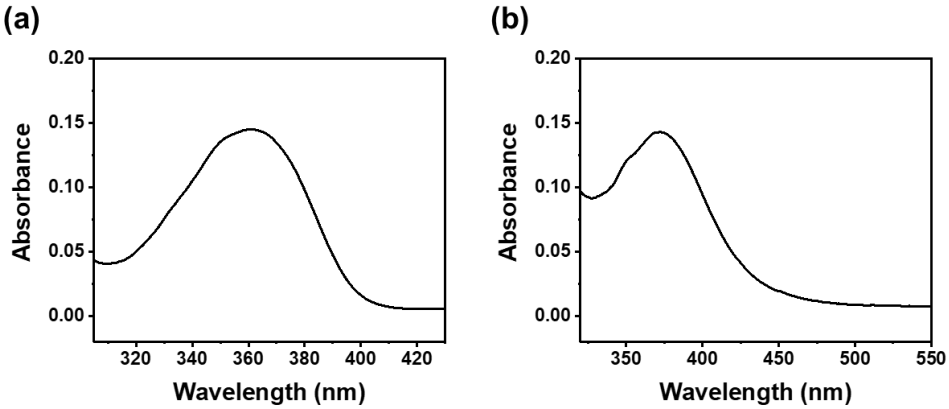

Figure S19. Absorption spectra of (a) **Mt-NI-Alde** and (a) **Mt-NI-2**

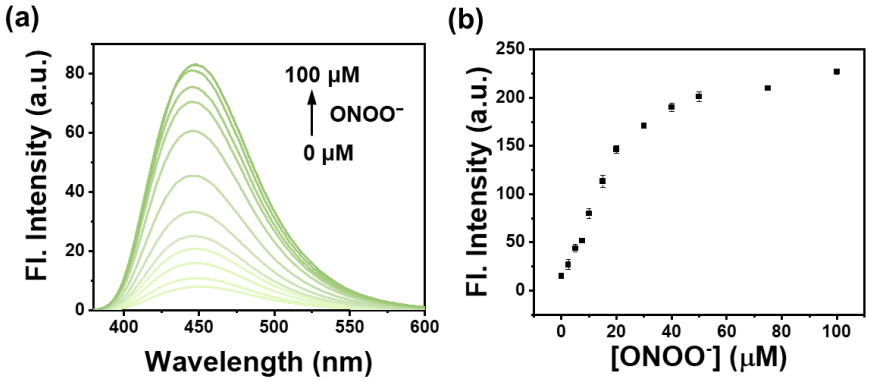

Figure S20. (a) Change in fluorescent intensity of **Mt-NI-1** (10 μM) with $ONOO^-$ (0-100 μM) (b) Plot of fluorescence intensity at 450 nm of **Mt-NI-1**, λ_{ex} = 361 nm.

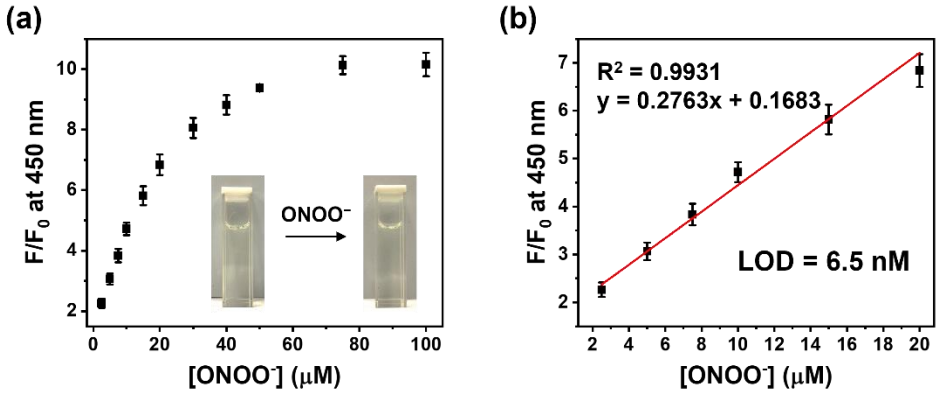

Figure S21. Titration of $ONOO^-$ with **Mt-NI-2** (a) The plot of changes in fluorescence according to concentrations of $ONOO^-$; Inset: optical change before and after addition of $ONOO^-$. (b) Parts of the plot of change in fluorescence according to concentrations of $ONOO^-$ between 2.5 μM to 20 μM as a linear range.

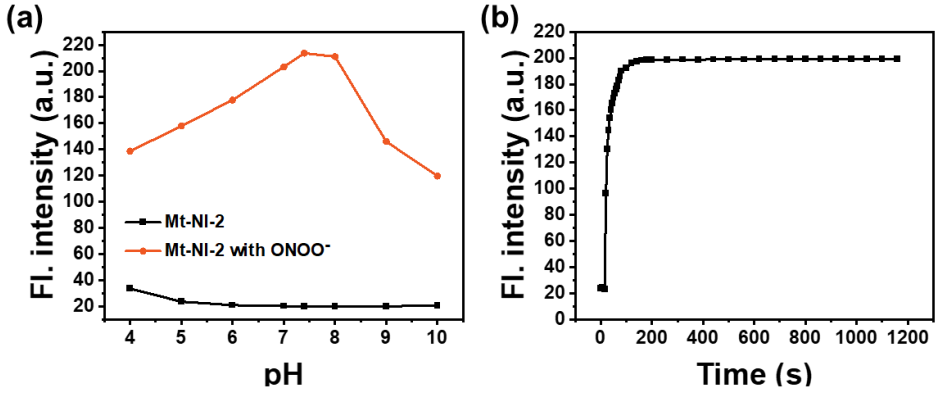

Figure S22. (a) Change in fluorescence intensity at 450 nm of **Mt-NI-2** (10 μM) in the absence or presence of $ONOO^-$ (50 μM) at various pH values. (b) Time-dependent fluorescent changes of **Mt-NI-2** (10 μM) upon addition of $ONOO^-$ (50 μM).

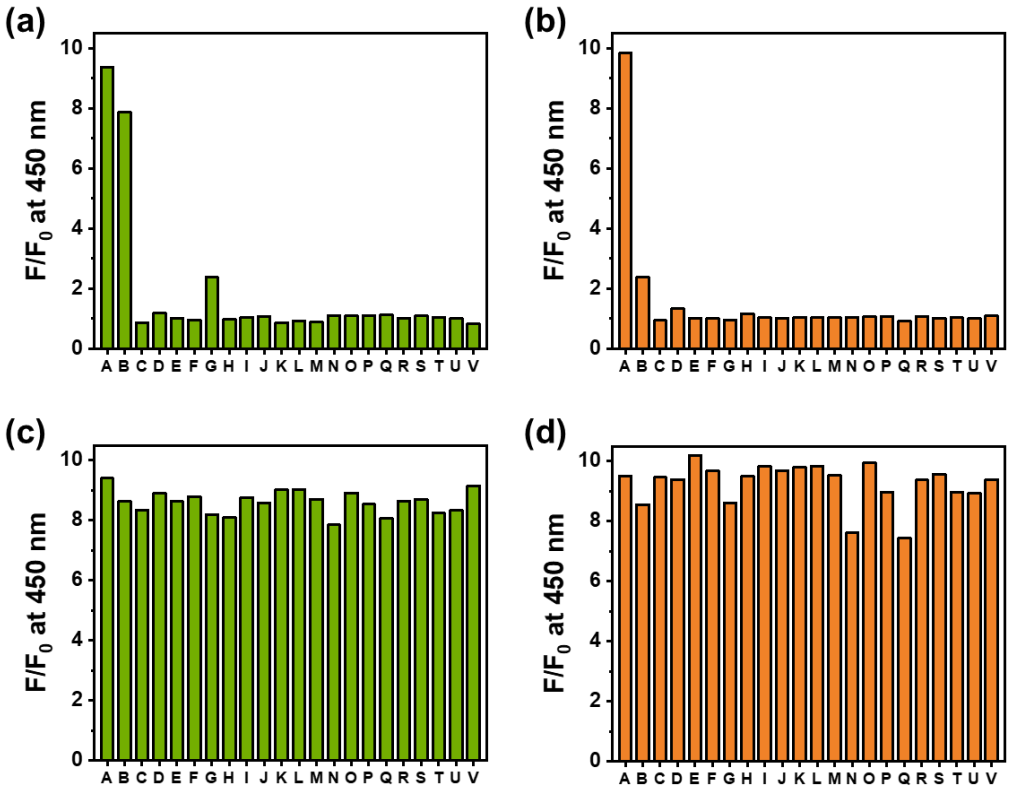

Figure S23. Change in fluorescence intensity of (a) **Mt-NI-1** (10 μM) and (b) **Mt-NI-2** (10 μM) in presence of (A) 50 μM of $ONOO^-$ and 250 μM of various relevant species (B) OCl^- (C) HO· (D) ROO· (E) TBHP (F) $^1O_2$ (G) $O_2^{\cdot-}$ (H) H_2O_2 (I) NO (J) NO_2^- (K) NO_3^- (L) Cl^- (M) HCO_3^- (N) $H_2PO_4^-$ (O) Mg^{2+} (P) Ca^{2+} (Q) Cu^{2+} (R) Fe^{2+} (S) L-Cys (T) Hcy (U) GSH (V) NaS in pH 7.4 PBS buffer. Change in fluorescence intensity of (c) **Mt-NI-1** (10 μM) and (d) **Mt-NI-2** (10 μM) in presence of (A) $ONOO^-$ only (50 μM) or 50 μM of $ONOO^-$ and 250 μM of various relevant species. Alphabets are the same as (a).

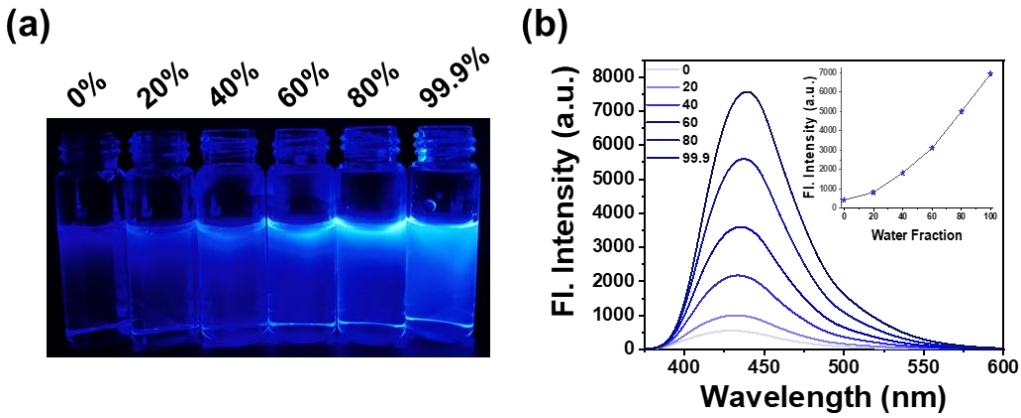

Figure S24. Fluorescence visualized image of **Mt-NI-Alde** in DMSO with different water fractions under 365 nm UV handheld lamp. Change in fluorescence intensity of the **Mt-NI-Alde** (10 μM) in DMSO with different water fractions, λ_{ex} = 361 nm.

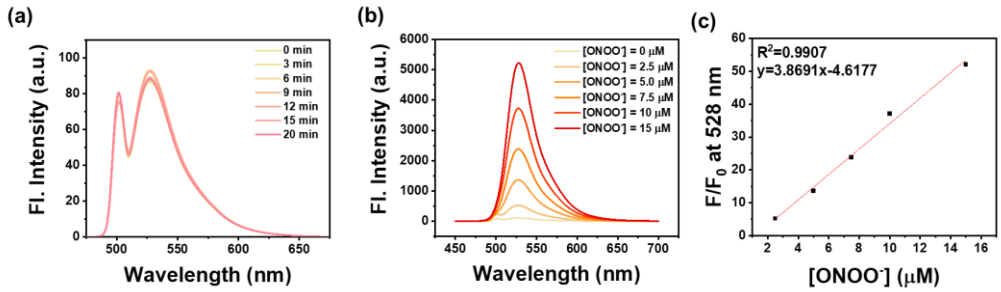

Figure S25. (a) Time-dependent fluorescence responses of DHR123 (10 μM) in PBS solution. (b) Fluorescent spectra of DHR123 (10 μM) with $ONOO^-$ titration (0-15 μM), λ_{ex} = 505 nm. (c) Plot of fluorescence intensity at 528 nm of DHR123, which corresponds to $ONOO^-$ concentration between 2.5 μM to 15 μM.

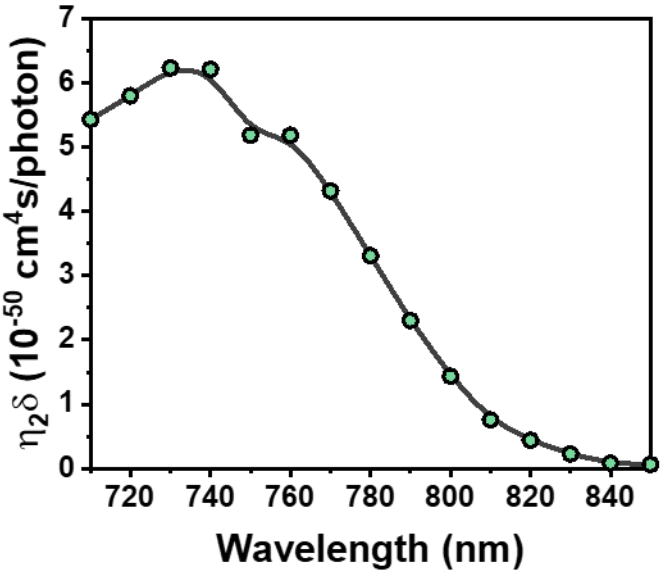

Figure S26. Two-photon fluorescence excitation spectra of **Mt-NI-2** (η_2: two-photon fluorescence quantum efficiency; δ: two-photon absorption cross section).

4. *In vitro* experiments

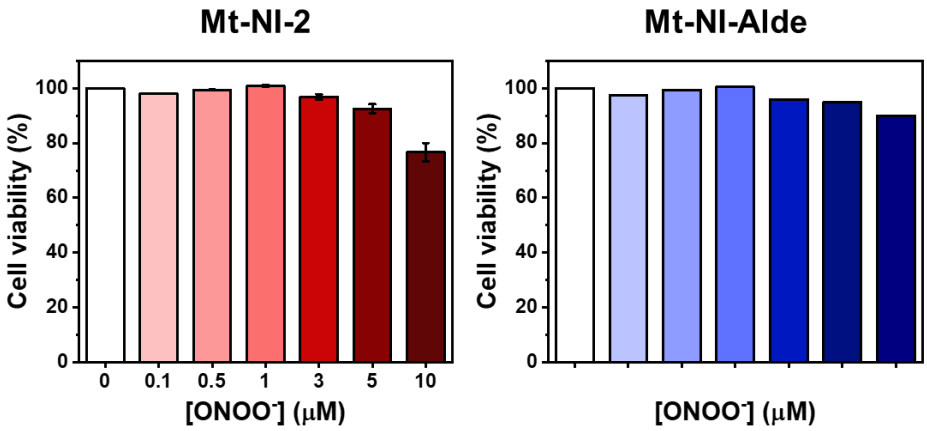

Figure S27. Cell viability of HeLa cells incubated with probe **Mt-NI-2** and its hydrolyzed form **Mt-NI-Alde** of different concentration (0, 0.1, 0.5, 1, 3, 5 or 10 μM) for 6 h.

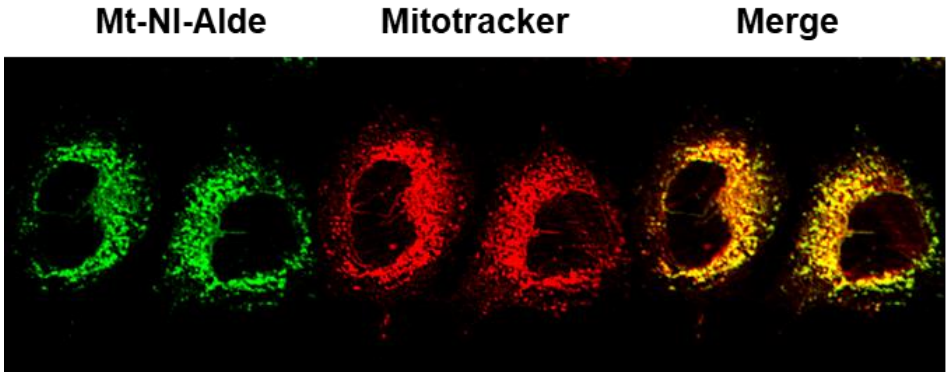

Figure S28. Fluorescence confocal images of HeLa cells costained with **Mt-NI-Alde** (5 μM, 30 min), and then MitoTracker Red FM (0.2 μM, 30 min). The image from the band path of 440–480 nm upon excitation of **Mt-NI-2** at 405 nm. For MitoTracker Red FM case, the excitation and emission bandpasses of the standard Cy5 filter set were used. Scale bar: 10 μm.

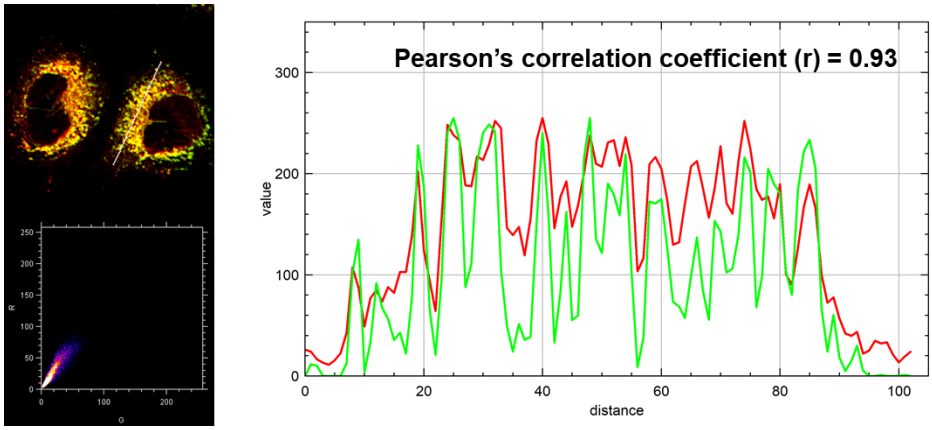

Figure S29. Co-location of **Mt-NI-2** (5 μM) and Mito-Tracker Red FM (0.2 μM) HeLa cells were first pre-treated with LPS (1 g·mL^{-1}) and IFN-γ (100 ng·mL^{-1}) for 4 h, followed by PMA (10 nM).

Table 1. Comparison list-up table of the representative $ONOO^-$ probes and Mt-NI-1 in this work.

No.	Probe Name	Chemical Structure	M. W. (g/mol)	$\lambda_{ex}/\lambda_{em}$ (nm)	Condition	Linear range	LOD	[Ref]
1	PNCy3Cy5	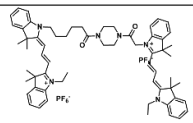	1227.23	530/660	0.1 M PBS (pH 7.4, 0.2% DMF, v/v)	0-0.7 μM	0.65 nM	[7]
2	MITO-CC	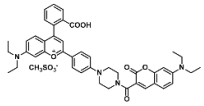	820.95	420/473	PBS/EtOH (pH 7.4, v/v, 7/3)	0-7.5 μM	11.3 nM	[8]
3	Probe 1	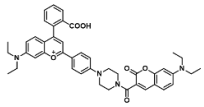	718.69	450/550	PBS (pH 7.4, 0.1 M 1% DMSO)	n.d.	184 nM	[9]
4	CC-ONOO	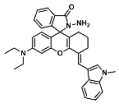	530.66	640/698	PBS (pH 7.4, 20% of CH_3CN, v/v)	0-30 μM	25 nM	[10]
5	Lyso-NA	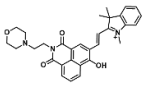	510.60	430/510	CPBS (pH 5.0, 50% ethanol)	0-140 μM	0.24 nM	[11]
6	BP-PN	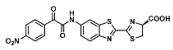	456.45	375/525	PBS (10 mM, pH 7.4) with 10 mM $MgCl_2$ at 37 °C	0.5-10 μM	200 nM	[12]
7	DCIPP	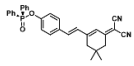	490.53	527/665	H_2O/DMSO solution (1:1, v/v, 10 mM PBS, pH 7.4)	0-15 μM	33 nM	[13]
8	BC-PN-2		303.36	450/520	PBS (pH 7.4, 50% DMSO)	7-17 μM	18 nM	[14]
9	LW-OTf	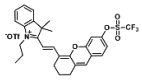	693.67	675/710	PBS (10 mM, pH 7.4)	0–4.2 μM	38.2 nM	[15]
10	BICBzBF	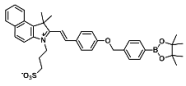	651.62	345/538	PBS (10 mM, 1% DMSO	0−15 μM	0.27 μM	[16]
11	HD-Bpin	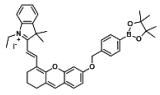	741.51	360/460	PBS (pH 7.2)	n.d.	0.28 uM	[17]
12	K-ONOO	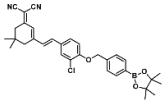	540.89	525/678	PBS (10 mM, pH 7.4, 1.5 mM CTAB)	0–15 μM	212 nM	[18]

No.	Probe Name	Chemical Structure	M. W. (g/mol)	$\lambda_{ex}/\lambda_{em}$ (nm)	Condition	Linear range	LOD	[Ref]
13	Mito-HC-TZ	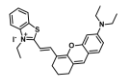	570.53	560/620,760	PBS (10 mM, pH 7.4, 50% DMSO)	0–100 μM	210 nM	[19]
14	BICBzDP	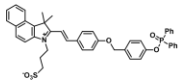	741.83	549/576	PBS (pH 7.4, 1% DMSO)	0–8 μM	47.8 nM	[20]
15	NRho	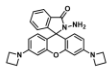	424.49	530/579	PBS (pH 7.4)	0–100 μM	2.45 μM	[21]
16	W-3a	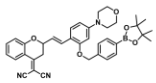	615.53	613/710	PBS (10 μM, pH 7.4, 50% DMSO)	0–18 μM	85 nM	[22]
17	Rd700-PN	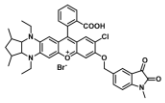	785.12	570/702	PBS(0.5% DMF)	1–10 μM	16.5 nM	[23]
18	HCy-OH-mito	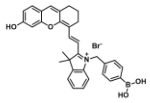	584.31	630/715	PBS (10 mM, pH 7.4)	0−1 μM	11.5 nM	[24]
19	Rh-3	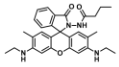	498.62	530/561	PBS (pH 7.4, 20% DMF)	2−18 μM	21 nm	[25]
20	HBT-FI-BnB	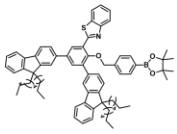	940.09	340/396	PBS (10 μM, pH 7.4, 5% THF, 0.2% Tween 80)	0−25 μM	2.1 μM	[26]
21	Mt-NI-2	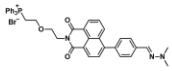	756.67	361/450	PBS (10 μM, pH 7.4)	0–20 μM	6.5 nM	This work

5. References

1. A. C. Sedgwick, H. H. Han, J. E. Gardiner, S. D. Bull, X. P. He and T. D. James, *Chem. Commun.*, 2017, **53**, 12822-12825.
2. W. W. Wang, J. H. Xiong, X. J. Song, Z. Wang, F. Zhang and Z. Q. Mao, *Anal. Chem.*, 2020, **92**, 13305-13312.
3. N. Meher, S. Panda, S. Kumar and P. K. Iyer, *Chem. Sci.*, 2018, **9**, 3978-3985.
4. L. Y. Chen, S. J. Park, D. Wu, H. M. Kim and J. Yoon, *Chem. Commun.*, 2019, **55**, 1766-1769.
5. C. T. Lee, W. T. Yang and R. G. Parr, *Phys. Rev. B*, 1988, **37**, 785-789.
6. A. D. Mclean and G. S. Chandler, *J. Chem. Phys.*, 1980, **72**, 5639-5648.
7. X. T. Jia, Q. Q. Chen, Y. F. Yang, Y. Tang, R. Wang, Y. F. Xu, W. P. Zhu and X. H. Qian, *J. Am. Chem. Soc.*, 2016, **138**, 10778-10781.
8. D. Cheng, Y. Pan, L. Wang, Z. B. Zeng, L. Yuan, X. B. Zhang and Y. T. Chang, *J. Am. Chem. Soc.*, 2017, **139**, 285-292.
9. D. Lee, C. S. Lim, G. Ko, D. Kim, M. K. Cho, S. J. Nam, H. M. Kim and J. Yoon, *Anal. Chem.*, 2018, **90**, 9347-9352.
10. D. D. Liu, S. M. Feng and G. Q. Feng, *Sens. Actuator B-Chem.*, 2018, **269**, 15-21.
11. B. P. Guo, J. Jing, L. X. Nie, F. Y. Xin, C. C. Gao, W. Yang and X. L. Zhang, *J. Mater. Chem. B*, 2018, **6**, 580-585.
12. J. B. Li, L. L. Chen, Q. Q. Wang, H. W. Liu, X. X. Hu, L. Yuan and X. B. Zhang, *Anal. Chem.*, 2018, **90**, 4167-4173.
13. R. Q. Yuan, Y. H. Ma, J. Y. Du, F. X. Meng, J. J. Guo, M. Hong, Q. L. Yue, X. Li and C. Z. Li, *Anal. Methods*, 2019, **11**, 1522-1529.
14. Y. Fang, R. X. Chen, H. F. Qin, J. J. Wang, Q. Zhang, S. J. Chen, Y. H. Wen, K. P. Wang and Z. Q. Hu, *Sens. Actuator B-Chem.*, 2021, **334**, 129603.
15. L. L. Wu, J. H. Liu, X. Tian, R. R. Groleau, S. D. Bull, P. Li, B. Tang and T. D. James, *Chem. Sci.*, 2021, **12**, 3921-3928.

16. P. M. Sonawane, T. Yudhistira, M. B. Halle, A. Roychaudhury, Y. Kim, S. S. Surwase, V. K. Bhosale, J. Kim, H. S. Park, Y. C. Kim, C. H. Kim and D. G. Churchill, *Dyes Pigment.*, 2021, **191**, 109371.
17. H. R. Bolland, E. M. Hammond and A. C. Sedgwick, *Chem. Commun.*, 2022, **58**, 10699-10702.
18. H. Kang, W. Shu, J. Yu, M. X. Gao, R. B. Han, J. Jing, R. B. Zhang and X. L. Zhang, *Sens. Actuator B-Chem.*, 2022, **359**, 131393.
19. Q. Q. Liu, C. Dong, J. Zhang, B. Zhao, Y. Q. Zhou, C. H. Fan and Z. L. Lu, *Dyes Pigment.*, 2023, **210**, 111045.
20. P. M. Sonawane, W. Lee, Y. Kim, A. Roychaudhury, V. K. Bhosale, D. Kim, H. S. Park, C. H. Kim and D. G. Churchill, *Spectrochim. Acta A Mol. Biomol. Spectrosc.*, 2022, **267**, 120568.
21. G. L. Wu, Z. H. Li, P. Huang and W. Y. Lin, *J. Mater. Chem. B*, 2024, **12**, 3436-3444.
22. X. Wang, X. C. Wang, Z. X. Bai, K. Q. Du, J. L. Zhang and Q. X. Han, *Talanta*, 2024, **270**, 125581.
23. J. K. Gong, X. Y. Wang, H. E. Fan, J. X. Wang, F. Zhang and Z. Q. Mao, *Talanta*, 2024, **267**, 125216.
24. X. W. Y. Liu, N. Fu, G. Wang, *Dyes Pigment.*, 2024, **225**, 112102.
25. S. J. Li, A. H. Mehmood, X. C. Tang, T. Yue and B. L. Dong, *Anal. Methods*, 2024, **16**, 1409-1414.
26. Z. K. Wang, M. Yan, M. M. Yu, G. Zhang, W. W. Fang and F. B. Yu, *Anal. Chem.*, 2024, **96**, 3600-3608.